

Hydrothermal Synthesis and Structural Characterization of Two New Three-Dimensional Oxyfluorinated Titanium Phosphates $\text{Ti}_4(\text{HPO}_4)_2(\text{PO}_4)_4\text{F}_2 \cdot \text{C}_4\text{N}_2\text{H}_{12} \cdot \text{H}_2\text{O}$ and $\text{Ti}_4(\text{HPO}_4)_2(\text{PO}_4)_4\text{F}_2 \cdot \text{C}_2\text{N}_2\text{H}_{10} \cdot \text{H}_2\text{O}$

Yunlong Fu, Yunling Liu, Zhan Shi, Yongcun Zou, and Wenqin Pang¹

State Key Laboratory of Inorganic Synthesis and Preparative Chemistry, Jilin University, Changchun 130023, China

E-mail: wqpang@mail.jlu.edu.cn

Received April 24, 2001; in revised form August 3, 2001; accepted August 16, 2001

Two new organo-templated three-dimensional fluorinated titanium phosphates $\text{Ti}_4(\text{HPO}_4)_2(\text{PO}_4)_4\text{F}_2 \cdot \text{C}_4\text{N}_2\text{H}_{12} \cdot \text{H}_2\text{O}$ **1** and $\text{Ti}_4(\text{HPO}_4)_2(\text{PO}_4)_4\text{F}_2 \cdot \text{C}_2\text{N}_2\text{H}_{10} \cdot \text{H}_2\text{O}$ **2** have been prepared hydrothermally in the presence of piperazine ($\text{C}_4\text{N}_2\text{H}_{10}$) and ethylenediamine ($\text{C}_2\text{N}_2\text{H}_8$) as templates, respectively. The as-synthesized products are characterized by powder X-ray diffraction, IR spectroscopy, and thermogravimetric and differential thermal analyses (TG-DTA). The structures have been solved by single-crystal X-ray diffraction analysis. The compound **1** crystallized in the monoclinic space group $C2/c$ (no. 15), with $M = 907.61$ g/mol, $a = 16.6549(17)$ Å, $b = 6.3378(6)$ Å, $c = 22.208(2)$ Å, $\beta = 94.862(4)^\circ$, $V = 2335.7(4)$ Å³, $Z = 4$, $R_1[I > 2\sigma(I)] = 0.0393$, $wR_2[I > 2\sigma(I)] = 0.1071$ and the compound **2** in the monoclinic space group $C2/m$ (no. 12), with $M = 880.56$ g/mol, $a = 16.6324(14)$ Å, $b = 6.3219(6)$ Å, $c = 11.0725(10)$ Å, $\beta = 94.362(2)^\circ$, $V = 1160.88(18)$ Å³, $Z = 2$, $R_1[I > 2\sigma(I)] = 0.0461$, $wR_2[I > 2\sigma(I)] = 0.1403$. They have similar three-dimensional frameworks built up from TiO_6 , TiO_5F octahedral, PO_4 , and $\text{PO}_3(\text{OH})$ tetrahedral units. There exist two types of 8-membered ring channels along the b axis in which the diprionated piperazine or ethylenediamine molecules are entrapped and along the c axis in which water molecules are entrapped. © 2001 Academic Press

Key Words: hydrothermal synthesis; crystal structure; titanium phosphates.

INTRODUCTION

Since the discovery of crystalline aluminophosphates (1–3) with ordered micropores, a large number of new metal phosphates with an open framework have been synthesized and reported, and the metal elements distribute from main group elements to transition metal elements (4), especially molybdenum (5), zirconium (6), and hafnium (7). One of the most important reasons for this is the potential application

in catalysis, adsorption, ionic conduction, ion exchange, electronics, and opto-electronics.

Similarly, hydrothermally synthesized titanium phosphates with open framework or layered structures also attract much attention as potential materials based on the same reasons. For example, the well-known α - $\text{Ti}(\text{HPO}_4)_2 \cdot \text{H}_2\text{O}$ (8, 9) and γ - $\text{Ti}(\text{H}_2\text{PO}_4)(\text{PO}_4) \cdot 2\text{H}_2\text{O}$ (10) have been investigated extensively for their ion-exchange properties and for their use in preparing organically or inorganically pillared materials. Potassium titanyl phosphate KTP (KTiOPO_4) has attracted considerable attention because of its excellent optical properties and low phase matching temperature sensitivity (11, 12). Recently, a few titanium phosphate compounds with an open framework structure have been synthesized and structurally characterized. Three new layered titanium phosphates with formula $\text{TiO}(\text{OH})(\text{H}_2\text{PO}_4) \cdot 2\text{H}_2\text{O}$ (13), $\text{Ti}_2\text{O}_3(\text{H}_2\text{PO}_4)_2 \cdot 2\text{H}_2\text{O}$ (14), and β - $\text{Ti}(\text{PO}_4)(\text{H}_2\text{PO}_4)$ (15) were prepared. Poojary *et al.* reported the synthesis and structures of three porous titanium phosphates $\text{Ti}_3(\text{PO}_4)_4(\text{H}_2\text{O})_2 \cdot \text{NH}_3$, $\text{Ti}_2\text{O}(\text{PO}_4)_2(\text{H}_2\text{O})_2$, and $(\text{NH}_4)_2\text{Ti}_3\text{O}_2(\text{HPO}_4)_2(\text{PO}_4)_2$ (16), and an organically templated mixed-valent $\text{Ti}^{\text{III}}/\text{Ti}^{\text{IV}}$ phosphate $\text{Ti}^{\text{III}}\text{Ti}^{\text{IV}}(\text{PO}_4)(\text{HPO}_4)_2(\text{H}_2\text{O})_2 \cdot 0.5\text{NH}_2\text{CH}_2\text{CH}_2\text{CH}_2\text{NH}_2$ with an open framework was also discovered (17). Ferey and co-workers reported the synthesis and *ab initio* structure determination of a new three-dimensional mixed-valence oxyfluorinated titanium phosphate MIL-15 $\text{Ti}^{\text{III}}\text{Ti}^{\text{IV}}(\text{PO}_4)_2 \cdot 2\text{H}_2\text{O}$ (MIL-15), two layered oxyfluorinated titanium phosphates $\text{Ti}_2(\text{PO}_4)_2\text{F}_4 \cdot \text{C}_2\text{N}_2\text{H}_{10}$ (MIL-6) and $\text{Ti}_2(\text{PO}_4)_2\text{F}_4 \cdot \text{C}_3\text{N}_2\text{H}_{12} \cdot \text{H}_2\text{O}$ (18, 19), and $\text{Ti}_6\text{O}_3(\text{H}_2\text{O})_3(\text{PO}_4)_7 \cdot (\text{H}_3\text{O})_3 \cdot (\text{H}_2\text{O})$ (MIL-18) (20).

In recent years, we have devoted effort toward hydrothermal and solvothermal synthesis in titanium-containing systems to obtain possible new types of materials with valuable properties: silica-pillared γ - TiPO (21), 2-D $[\text{H}_3\text{NC}_2\text{H}_4\text{NH}_2]\text{TiOPO}_4$ (22), 3-D $\text{Ti}_2(\text{HPO}_4)_3(\text{PO}_4) \cdot 0.5\text{C}_4\text{N}_2\text{H}_{12}$ and $\text{Ti}_7(\text{HPO}_4)_6(\text{PO}_4)_6 \cdot \text{C}_6\text{N}_2\text{H}_{14}$ (23), and 1-D chiral $\text{Ti}_3\text{P}_6\text{O}_{27} \cdot 5\text{NH}_3\text{CH}_2\text{CH}_2\text{NH}_3 \cdot 2\text{H}_3\text{O}$ (24).

¹To whom correspondence should be addressed.



In this paper, we report the synthesis and characterization of two new three-dimensional oxyfluorinated and organo-templated titanium phosphates $\text{Ti}_4(\text{HPO}_4)_2(\text{PO}_4)_4\text{F}_2 \cdot \text{C}_4\text{N}_2\text{H}_{12} \cdot \text{H}_2\text{O}$ **1** and $\text{Ti}_4(\text{HPO}_4)_2(\text{PO}_4)_4\text{F}_2 \cdot \text{C}_2\text{N}_2\text{H}_{10} \cdot \text{H}_2\text{O}$ **2**.

EXPERIMENTAL

Synthesis and Characterization

The title compounds were hydrothermally prepared from a mixture of titanium powder (99%, Shanghai Chemical Reagent Factory), phosphoric acid (85 wt%, Beijing Chemical Plant), piperazine or ethylenediamine (99.0%, Beijing Chemical Plant), hydrogen fluoride (40 wt%, Beijing Chemical Plant), and distilled water in the molar ratios 1:15:1:3:30 for compound **1** and 1:15:1:6:30 for compound **2**. The mixture was sealed in a Teflon-lined stainless-steel autoclave and heated at 240°C for 5 days under auto-genous pressure. The resulting crystals were recovered by typical filtration, washed thoroughly with distilled water, and dried at room temperature.

The powder X-ray diffraction (XRD) patterns were recorded (Bragg–Brentano) on a Siemens D5005 diffractometer by using $\text{CuK}\alpha$ radiation ($\lambda = 1.5418 \text{ \AA}$) with a graphite monochromator. The step size was 0.02° and the count time was 4 s. The element analyses were performed on a Perkin–Elmer 2400 element analyzer and the inductively coupled plasma (ICP) analysis on a Perkin–Elmer Optima 3300 DV ICP spectrometer. The IR spectrum was obtained on a Nicolet Impact 410 FTIR spectrometer using KBr pellets. The thermogravimetric analysis (TGA) and the differential thermal analysis (DTA) were conducted on a Perkin–Elmer TGA 7 thermogravimetric analyzer and a Perkin–Elmer DTA 1700 differential thermal analyzer, respectively, in air with a heating rate of $10^\circ\text{C min}^{-1}$.

Determination of Crystal Structure

For **1**, a colorless plate-like crystal with dimensions of $0.40 \times 0.06 \times 0.06 \text{ mm}^3$ was selected and mounted on a glass fiber by using cyanoacrylate. The data collection and the structural analysis were performed on a Siemens Smart CCD diffractometer with graphite-monochromated $\text{MoK}\alpha$ ($\lambda = 0.71073 \text{ \AA}$) radiation. A total of 9115 reflections were collected, of which 3362 were unique ($R_{\text{int.}} = 0.0914$) and 2560 were considered to be observed with $I > 2\sigma(I)$. The data processing was accomplished with the SAINT processing program (25). The structure was solved by direct methods and refined by full-matrix least squares on F^2 using SHELXTL Version 5.1 (26). All nonhydrogen atoms were refined anisotropically. The hydrogen atoms of the amine molecule were placed geometrically ($d_{\text{N-H}} = 0.90 \text{ \AA}$, $d_{\text{C-H}} = 0.97 \text{ \AA}$), and allowed to ride on the atoms to which they were attached with fixed isotropic thermal parameters.

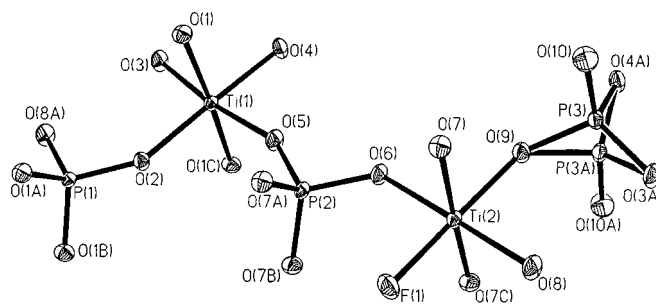


FIG. 1. ORTEP (29) view of the structure of **2** showing the atom-labeling scheme (50% thermal ellipsoids).

The remaining H atoms (those of the water molecule and the P(–OH) group) were located by difference Fourier analysis.

For **2**, based on the same process, a rod-like crystal with dimensions of $0.20 \times 0.08 \times 0.08 \text{ mm}^3$ was selected. A total of 4781 reflections were collected, of which 1817 were unique ($R_{\text{int.}} = 0.0351$) and 1305 were considered to be observed with $I > 2\sigma(I)$. All nonhydrogen atoms were refined anisotropically. The hydrogen atoms of the amine molecule were not located due to the disorder. Atoms P(3), O(10), O(1W), C(1), and N(1) are disordered over two positions with equal occupancy as depicted in Fig. 1. The experimental X-ray data are listed in Table 1. The atomic coordinates with isotropic temperature factors and selected bond lengths for **1** and **2** are given in Tables 2 and 3, respectively.

RESULTS AND DISCUSSION

Synthesis and Characterization

The composition of the reaction mixture and the crystallization conditions for **1** and **2** are presented in Table 4. It is seen that the formation of the titanium phosphates was markedly influenced by the molar ratio of $\text{H}_3\text{PO}_4/\text{H}_2\text{O}$. The concentration of HF mainly affected the rates of nucleation and crystal growth. When the time was lengthened, a new phase mixed with the title compound appeared in the powder XRD of the products.

Because of the structural similarity of the two compounds, both of them show almost the same diffracting positions of XRD. The powder XRD patterns of the two compounds with that simulated (27) on the basis of the single-crystal structure are presented in Fig. 2. The diffraction peaks on both patterns correspond well in position, indicating the phase purity of the as-synthesized sample. The differences in reflection intensity are probably due to the preferred orientation in the powder samples. The ICP analysis and elemental analysis are in good agreement with the theoretical values: for **1**, Ti, 21.00 wt%; P, 20.50 wt%; C, 5.35 wt%; H, 1.71 wt%; N, 3.15 wt% (calculated: Ti, 21.10 wt%; P, 20.47 wt%; C, 5.29 wt%, H, 1.78 wt%, N, 3.09

TABLE 1
Crystal Data and Structure Refinement for 1 and 2

Empirical formula	Ti ₄ (HPO ₄) ₂ (PO ₄) ₄ F ₂ · C ₄ N ₂ H ₁₂ · H ₂ O	Ti ₄ (HPO ₄) ₂ (PO ₄) ₄ F ₂ · C ₂ N ₂ H ₁₀ · H ₂ O
Formula weight	907.61	880.56
Temperature	293(2) K	293(2) K
Wavelength	0.71073 Å	0.71073 Å
Crystal system	Monoclinic	Monoclinic
Space group	C2/c	C2/m
Unit cell dimensions	<i>a</i> = 16.6549(17) Å <i>b</i> = 6.3378(6) Å <i>c</i> = 22.208(2) Å <i>β</i> = 94.862(4)°	<i>a</i> = 16.6324(14) Å <i>b</i> = 6.3219(6) Å <i>c</i> = 11.0725(10) Å <i>β</i> = 94.362(2)°
Volume	2335.7(4) Å ³	1160.88 (18) Å ³
Z	4	2
Density (calculated)	2.581 Mg/m ³	2.519 Mg/m ³
Absorption coefficient	1.868 mm ⁻¹	1.875 mm ⁻¹
<i>F</i> (000)	1800	870
Crystal size	0.40 × 0.06 × 0.06 mm ³	0.20 × 0.08 × 0.08 mm ³
<i>θ</i> range for data collection	1.84°–30.07°	1.84°–30.01°
Limiting indices	–23 ≤ <i>h</i> ≤ 17, –8 ≤ <i>k</i> ≤ 8, –30 ≤ <i>l</i> ≤ 23	–21 ≤ <i>h</i> ≤ 23, –8 ≤ <i>k</i> ≤ 8, –15 ≤ <i>l</i> ≤ 11
Reflections collected / unique	9115/3362 [<i>R</i> (int) = 0.0914]	4781/1817 [<i>R</i> (int) = 0.0351]
Completeness to <i>θ</i> = 30.07	98.0%	98.6%
Absorption correction	Empirical	Empirical
Max. and min. transmission	0.8961 and 0.5219	0.8644 and 0.7055
Refinement method	Full-matrix least-squares on <i>F</i> ²	Full-matrix least-squares on <i>F</i> ²
Data/restraints/parameters	3362/0/204	1817/13/129
Goodness-of-fit on <i>F</i> ²	1.057	1.062
Final <i>R</i> indices [<i>I</i> > 2σ(<i>I</i>)] ^a	<i>R</i> ₁ = 0.0393, w <i>R</i> ₂ = 0.1071	<i>R</i> ₁ = 0.0461, w <i>R</i> ₂ = 0.1403
<i>R</i> indices (all data)	<i>R</i> ₁ = 0.0544, w <i>R</i> ₂ = 0.1148	<i>R</i> ₁ = 0.0692, w <i>R</i> ₂ = 0.1516
Largest diff. peak and hole	0.724 and –0.935 e · Å ⁻³	1.540 and –1.110 e · Å ⁻³

$$^a R_1 = \sum ||F_o| - |F_c|| / \sum |F_o|. \quad wR_2 = [\sum (w(F_o^2 - F_c^2)^2) / \sum (w(F_o^2)^2)]^{1/2}.$$

wt%), and for **2**, Ti, 21.85 wt%; P, 21.21 wt%; C, 3.04 wt%; H, 1.60 wt%; N, 2.95 wt% (calculated: Ti, 21.74 wt%; P, 21.10 wt%; C, 2.93 wt%, H, 1.48 wt%, N, 3.08 wt%).

The IR spectra of the compounds (Fig. 3) clearly show the existence of organic amine (three typical sharp peaks for piperazine at 1587, 1467, and 1424 cm⁻¹, two typical sharp peaks for ethylenediamine at 1517 and 1608 cm⁻¹) and the broad bands at around 1000 cm⁻¹ are associated with the asymmetric stretching vibrations of PO₄ units. Two (compound **1**) or three (compound **2**) absorption peaks also appear at about 550 cm⁻¹ due to bending vibrations of phosphate groups. The broadbands observed at around 3040 and 3100 cm⁻¹ correspond to the combination and overlapping of stretching vibrations of N–H, C–H, and O–H.

Thermogravimetric analysis of **1** (Fig. 4) shows that total weight loss of 18.0% (calculated: 17.7%) at 350–750°C corresponds to the loss of crystal water, condensation due to the removal of H₂O and HF. The DTA curve exhibits two exothermic peaks at approximately 460 and 510°C, corresponding to the decomposition of the template, condensation due to the removal of H₂O and HF. In addition to a pattern of weight loss similar to that above of 350°C, the TG-DTA of **2** (shown in Fig. 4) shows weight loss of approx-

imately 3.50% and an endothermic peak at 100–260°C because of the loss of crystal water (calculated 2.1%). The structures of the two compounds collapse and convert to amorphous phases after calcination at 600°C for 2 h. At 800°C the amorphous phase recrystallizes to form TiP₂O₇ phases (JCPDS: 38-1468) as a main ingredient with some other phase as confirmed by powder X-ray diffraction.

Description of Structure

Due to the similar inorganic framework structures of the two compounds, the compound **1** is chosen as a model for structural description. The asymmetric unit of **1** is shown in Fig. 5. It contains two crystallographically distinct Ti atoms in which Ti1 is coordinated to five oxygen atoms and one terminal fluorine atom and Ti2 is coordinated to six O atoms. The Ti–F bond length and the F–Ti–O angles are 1.8506(17) Å and 89.16(8)°–179.45(7)° respectively. The Ti–O bond lengths and O–Ti–O bond angles are in the range 1.8795(6)–1.9695(5) Å and 86.7(2)°–177.3(2)°, respectively, which are in good agreement with those reported previously for other titanium phosphates. Of the three crystallographically distinct P atoms, P(2), which has one terminal hydroxyl group characterized by the longer P–O

TABLE 2
Atomic Coordinates ($\times 10^4$) and Equivalent Isotropic Displacement Parameters ($\text{\AA}^2 \times 10^3$) for **1** and **2**

Atom	x	y	z	$U(\text{eq})^a$
Compound 1				
Ti(1)	2827(1)	70(1)	5753(1)	11(1)
Ti(2)	6405(1)	-22(1)	6989(1)	10(1)
P(1)	2306(1)	5016(1)	5691(1)	10(1)
P(2)	4424(1)	-724(1)	6669(1)	11(1)
P(3)	8044(1)	7(1)	7936(1)	9(1)
F(1)	1759(1)	158(2)	5446(1)	21(1)
O(1)	2876(1)	3121(3)	5772(1)	15(1)
O(2)	2485(1)	-17(3)	6538(1)	17(1)
O(3)	2826(1)	-2998(3)	5725(1)	15(1)
O(4)	3179(1)	102(3)	4928(1)	15(1)
O(5)	3948(1)	-46(3)	6080(1)	14(1)
O(6)	4050(1)	60(3)	7227(1)	17(1)
O(7)	4407(1)	-3182(3)	6638(1)	21(1)
O(8)	5288(1)	62(3)	6650(1)	15(1)
O(9)	6396(1)	3078(3)	7035(1)	14(1)
O(10)	6404(1)	-3045(3)	7030(1)	15(1)
O(11)	6716(1)	33(3)	6186(1)	16(1)
O(12)	7499(1)	19(3)	7344(1)	13(1)
N(1)	560(2)	-493(5)	4578(1)	38(1)
C(1)	167(2)	-2177(6)	4904(2)	44(1)
C(2)	44(2)	1391(7)	4498(2)	45(1)
O(1W)	5000	-5592(5)	7500	22(1)
Compound 2				
Ti(1)	6411(1)	-5000	13996(1)	10(1)
Ti(2)	7167(1)	-5000	8504(1)	10(1)
P(1)	8043(1)	-5000	15864(1)	9(1)
P(2)	7318(1)	-5000	11388(1)	10(1)
P(3)	5571(1)	-4289(3)	6691(2)	11(1)
F(1)	8234(2)	-5000	9104(3)	21(1)
O(1)	6398(2)	-1936(4)	14076(3)	15(1)
O(2)	7508(2)	-5000	14677(3)	13(1)
O(3)	5938(2)	-5000	15564(4)	18(1)
O(4)	5295(2)	-5000	13270(4)	17(1)
O(5)	6719(2)	-5000	12376(4)	16(1)
O(6)	6825(2)	-5000	10158(3)	14(1)
O(7)	7141(2)	-1947(4)	8498(3)	15(1)
O(8)	7506(2)	-5000	6907(4)	19(1)
O(9)	6040(2)	-5000	7856(4)	14(1)
O(10)	5567(4)	-1809(9)	6753(6)	22(1)
N(1)	4499(11)	0	902(17)	149(6)
C(1)	5080(20)	1680(50)	660(30)	162(13)
O(1W)	5000	562(13)	5000	25(2)

^a $U(\text{eq})$ is defined as one-third of the trace of the orthogonalized U_{ij} tensor.

bond distances P(2)-O(7), 1.560(2) Å, is connected to Ti(1) and Ti(2) through three bridging O atoms. The P(1) and P(3) atoms, each of which shares four oxygen atoms with adjacent Ti atoms with the P-O distances varying between 1.5237(19) and 1.5369(18) Å, are also connected to Ti(1) and Ti(2) through four bridging O atoms.

The framework structure of **1** is constructed from strictly alternating TiO_6 , TiO_5F octahedra, PO_4 , and $\text{PO}_3(\text{OH})$

tetrahedra. The 3-D open framework structure of **1** can be viewed as constructed from zigzag 2-D layers along the a axis: (i) the TiO_6 octahedra and the PO_4 or $\text{PO}_3(\text{OH})$ tetrahedra connect together to form infinite double layers with alternating 4-membered rings (4-MRs) and distorted 8-MRs along the a direction (Fig. 6a); (ii) the infinite double layers are linked together by sharing oxygen atoms to form 8-MR channels along the b axis (Fig. 6b); and (iii) further connections in the same way build up the three-dimensional framework with 8-MR main channels along the b axis and distorted 8-MR channels (relative to the main channels along the b axis) along the c axis (Fig. 6c). So, there are two types of intersecting 8-MR channels in the framework. Viewed along the b direction, each coupled Ti-F (terminal fluorine) bond located at opposite positions in the same channel points toward the channel center. A similar inorganic framework structure has been reported for the fluorinated zirconium phosphate compound (28).

The diprotonated piperazine molecules are trapped in the main 8-MR channels, and they interact with the oxygen and

TABLE 3
Selected Bond Lengths (Å) for **1** and **2**

Compound 1 ^a			
Ti(1)-F(1)	1.8506(17)	Ti(2)-O(11)	1.8987(19)
Ti(1)-O(2)	1.8795(19)	Ti(2)-O(10)	1.9178(17)
Ti(1)-O(1)	1.9357(17)	Ti(2)-O(12)	1.9236(18)
Ti(1)-O(3)	1.9456(17)	Ti(2)-O(8)	1.9480(19)
Ti(1)-O(5)	1.9456(18)	Ti(2)-O(6) # 1	1.9585(19)
Ti(1)-O(4)	1.9695(19)	Ti(2)-O(9)	1.9678(17)
P(1)-O(3) # 2	1.5257(18)	P(2)-O(6)	1.5154(19)
P(1)-O(1)	1.5315(17)	P(2)-O(8)	1.5262(18)
P(1)-O(11) # 3	1.5358(18)	P(2)-O(5)	1.5334(19)
P(1)-O(4) # 4	1.5365(19)	P(2)-O(7)	1.560(2)
P(3)-O(2) # 1	1.5237(19)	P(3)-O(9) # 5	1.5353(17)
P(3)-O(12)	1.5326(18)	P(3)-O(10) # 6	1.5369(18)
C(2)-C(1) # 7	1.489(6)		
Compound 2 ^b			
Ti(1)-O(5)	1.902(4)	Ti(2)-F(1)	1.847(3)
Ti(1)-O(2)	1.921(4)	Ti(2)-O(8)	1.896(4)
Ti(1)-O(1)	1.940(3)	Ti(2)-O(7)	1.930(3)
Ti(1)-O(3)	1.960(4)	Ti(2)-O(9)	1.955(4)
Ti(1)-O(4)	1.965(4)	Ti(2)-O(6)	1.958(4)
P(1)-O(8) # 1	1.513(4)	P(2)-O(7) # 3	1.525(3)
P(1)-O(2)	1.530(4)	P(2)-O(5)	1.534(4)
P(1)-O(1) # 2	1.535(3)	P(2)-O(6)	1.535(4)
P(3)-O(3) # 4	1.500(4)	P(3)-O(10)	1.569(6)
P(3)-O(4) # 5	1.513(4)	P(3)-O(9)	1.524(4)
C(1)-C(1) # 6	1.47(6)		

^aSymmetry transformations used to generate equivalent atoms: # 1, $-x + 1, y, -z + \frac{3}{2}$; # 2x, $y + 1, z$; # 3, $x - \frac{1}{2}, y + \frac{1}{2}, z$; # 4, $-x + \frac{1}{2}, -y + \frac{1}{2}, -z + 1$; # 5, $-x + \frac{3}{2}, y - \frac{1}{2}, -z + \frac{3}{2}$; # 6, $-x + \frac{3}{2}, y + \frac{1}{2}, -z + \frac{3}{2}$; # 7, $-x, -y, -z + 1$.

^bSymmetry transformations used to generate equivalent atoms: # 1, $x, y, z + 1$; # 2, $-x + \frac{3}{2}, -y - \frac{1}{2}, -z + 3$; # 3, $-x + \frac{3}{2}, -y - \frac{1}{2}, -z + 2$; # 4, $x, y, z - 1$; # 5, $-x + 1, -y - 1, -z + 2$; # 6, $-x + 1, y, -z$.

TABLE 4
Gel Composition and Crystallization Conditions for **1** and **2**

Run	Reactants (molar ratio)					Crystallization conditions		Product
	Ti	P ₂ O ₅	Templates	HF	H ₂ O	Time (days)	T (°C)	
1	1.0	7.5	1.0pip ^a	1.0–4.0	30	5	240	1
2	1.0	< 5	1.0pip	3.0	30	5	240	Unknown <i>a</i>
3	1.0	7.5	1.0pip	> 6.0	30	5	240	Unknown <i>b</i>
4	1.0	7.5	4.0pip	3.0	30	5	240	Unknown <i>a</i>
5	1.0	7.5	1.0pip	3.0	30	7	240	Unknown <i>c</i> + 1
6	1.0	7.5	1.0en ^a	1.0–6.0	30	5	240	2
7	1.0	< 5	1.0en	6.0	30	5	240	unknown <i>d</i>
8	1.0	7.5	4.0en	6.0	30	5	240	Unknown <i>d</i>
9	1.0	7.5	1.0en	> 7.0	30	5	240	Unknown <i>e</i>
10	1.0	7.5	1.0en	6.0	30	7	240	Unknown <i>f</i> + 2

^apip = piperazine, en = ethylenediamine.

fluorine attached to the framework through H bondings. The H bonding for **1** is listed in Table 5. Interestingly, the water molecules are trapped in the distorted 8-MR channel or between two 4-MR rings formed by TiO₆ octahedra and

PO₃(OH) tetrahedra viewed along the *b* axis. The shorter distances of O(1W)–H(1W) ⋯ O(9)#7 (2.7545(19) Å) and O(7)–H(7) ⋯ O(1W) (2.580(3) Å) suggest there are strong H-bond interactions between the trapped water molecules and part of the surrounding oxygen atoms.

Compound **2** has the same inorganic framework as that of **1**. Interestingly, the diprotonated ethylenediamine in compound **2** appears to assume a shape like piperazine due to the thermal disorder. This phenomenon shows a possible relationship between the structure described here and the shapes of organic templates, although it may need further research.

CONCLUSIONS

Two new organo-templated three-dimensional titanium phosphates have been prepared hydrothermally using

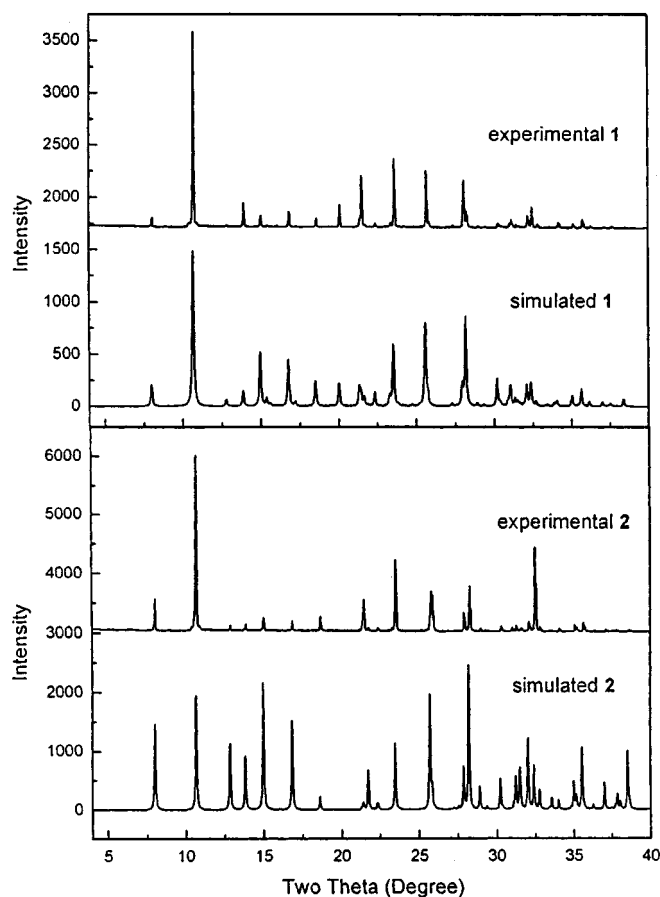


FIG. 2. Experimental and simulated powder X-ray diffraction patterns of **1** and **2**.

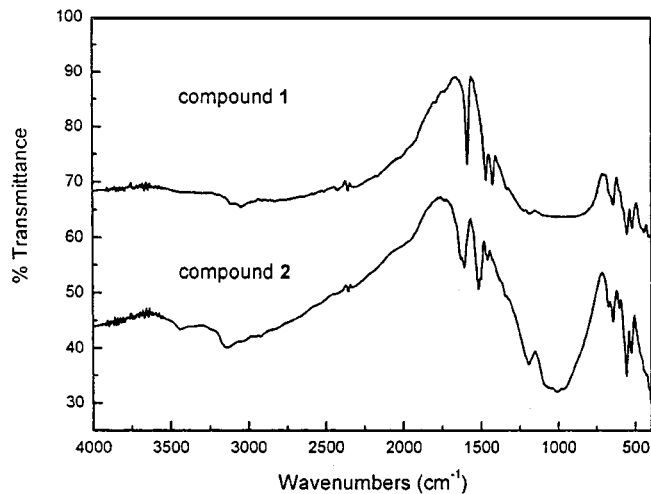


FIG. 3. IR spectra of **1** and **2**.

TABLE 5
Hydrogen Bonds for 1

<i>D</i> - <i>H</i> ... <i>A</i>	<i>d</i> (<i>D</i> - <i>H</i>) (Å)	<i>d</i> (<i>H</i> ... <i>A</i>) (Å)	<i>d</i> (<i>D</i> ... <i>A</i>) (Å)	Angle (<i>D</i> - <i>H</i> ... <i>A</i>) (°)
N(1)-H(1A)...F(1)	0.90	1.83	2.688(3)	157.3
N(1)-H(1A)...O(1)#1	0.90	2.62	3.161(3)	119.1
N(1)-H(1B)...O(7)#2	0.90	1.96	2.833(3)	163.6
O(1W)-H(1W)...O(9)#3	0.87(4)	2.00(4)	2.7545(19)	144(4)
O(1W)-H(1W)...O(6)#4	0.87(4)	2.52(4)	3.210(3)	137(3)
O(7)-H(7)...O(1W)	0.77(4)	1.82(4)	2.580(3)	169(4)

Note. Symmetry transformations used to generate equivalent atoms: #1, $-x + \frac{1}{2}$, $-y + \frac{1}{2}$, $-z + 1$; #2, $-x + \frac{1}{2}$, $-y - \frac{1}{2}$, $-z + 1$; #3, x , $y - 1$, z ; #4, $-x + 1$, $y - 1$, $-z + \frac{3}{2}$.

crucial for the formation of open framework oxyfluorinated titanium phosphates. The practical concentration of phosphoric acid in the described system is also an important factor in the formation of titanium phosphate with open framework.

ACKNOWLEDGMENTS

The authors gratefully acknowledge the financial support of the Ministry of Science and Technology of China through the State Basic Research Project (G200077507) and the National Natural Science Foundation of China (29871012, 29733070).

REFERENCES

- S. T. Wilson, B. M. Lok, C. A. Messina, T. R. Cannan, and E. M. Flanigen, *J. Am. Chem. Soc.* **104**, 1146 (1982).
- M. E. Davis, C. Saldarriaga, C. Montes, J. Garces, and C. Crowder, *Nature* **331**, 698 (1988).
- J. Chen, W. Pang, and R. Xu, *Topics in Catal.* **9**, 93 (1999).
- A. K. Cheetham, G. Férey, and T. Loiseau, *Angew. Chem. Int. Ed.* **39**, 3268 (1999).
- R. C. Haushalter and L. A. Mundi, *Chem. Mater.* **4**, 31 (1992).
- E. R. Losilla, M. A. G. Aranda, and S. Bruque, *J. Solid State Chem.* **125**, 261 (1996).
- M. A. Salvado, P. Pertierra, S. Garcia-Granda, J. R. Garcia, J. Rodriguez, M. T. Fernandez-Diaz, *Acta Crystallogr. Sect. B* **52**, 896 (1996), *Acta Crystallogr. Sect. B* **53**, 188 (1997).
- A. Clearfield and J. A. Stynes, *J. Inorg. Nucl. Chem.* **26**, 117 (1964).
- A. N. Christensen, E. K. Andersen, I. G. K. Andersen, G. Alberti, M. Nielsen, and M. S. Lehmann, *Acta Chem. Scand.* **44**, 865 (1990).
- S. Allulli, C. Ferragina, A. La. Ginestra, M. A. Massucci, and N. Tomassini, *J. Inorg. Nucl. Chem.* **39**, 1043 (1977).
- G. D. Stucky, M. L. F. Phillips, and T. E. Gier, *Chem. Mater.* **1**, 492 (1989).
- M. L. F. Phillips, W. T. A. Harrison, G. D. Stucky, E. M. McCarron III, J. C. Calabrese, and T. E. Gier, *Chem. Mater.* **4**, 222 (1992).
- Y. J. Li and M. S. Whittingham, *Solid State Ionics* **63**, 391 (1993).
- A. I. Bortun, L. N. Bortun, A. Clearfield, M. A. Villa-Garcia, J. R. Garcia, and J. Rodriguez, *J. Mater. Res.* **11**, 2490 (1996).
- A. M. Krogh Anderson, P. Norby, and T. Vogt, *Inorg. Chem.* **37**, 4313 (1998).
- D. M. Poojary, A. I. Bortun, and L. N. Bortun, A. Clearfield, *J. Solid State Chem.* **132**, 213 (1997).
- S. Ekambaram and S. Sevov, *Angew. Chem. Int. Ed.* **38**, 372 (1999).
- C. Serre and G. Férey, *J. Mater. Chem.* **9**, 579 (1999).
- C. Serre, N. Guillou, and G. Férey, *J. Mater. Chem.* **9**, 1185 (1999).
- C. Serre and G. Férey, *C. R. Acad. Sci. Paris Ser. II* **2**, 85 (1999).
- X. Jiao, D. Chen, W. Pang, R. Xu, and Y. Yue, *J. Mater. Chem.* **8**, 2831 (1998).
- Y. Zhao, G. Zhu, X. Jiao, W. Liu, and W. Pang, *J. Mater. Chem.* **10**, 463 (2000).
- Y. Liu, Z. Shi, L. Zhang, Y. Fu, J. Chen, B. Li, J. Hua, and W. Pang, *Chem. Mater.* **13**, 2017 (2001).
- Y. Guo, Z. Shi, J. Yu, J. Wang, Y. Liu, N. Bai, and W. Pang, *Chem. Mater.* **13**, 203 (2001).
- SMART and SAINT (software packages), Siemens Analytical X-ray Instruments Inc., Madison, WI, 1996.
- SHELXTL, Version 5.1, Siemens Industrial Automation, Inc., 1997.
- W. Kraus and G. Nolze, Powdercell for Windows, Version 1.0, Federal Institute for Materials Research and Testing, 1997.
- E. Kemnitz, M. Wloka, S. Trojanov, and A. Stiewe, *Angew. Chem. Int. Ed. Engl.* **35**, 2677 (1996).
- C. K. Johnson, Oak Ridge National Laboratory Report ORNL-5138, with local modifications, Oak Ridge, TN, 1976.